

Upper Limit on Flux of Cosmic-Ray Monopoles Obtained with a Three-Loop Superconductive Detector

B. Cabrera, M. Taber, R. Gardner, and J. Bourg

Physics Department, Stanford University, Stanford, California 94305

(Received 8 August 1983)

A three-loop superconductive monopole detector has been continuously operated for over 150 days. Its sensing area is 476 cm^2 (71 cm^2 loop area and 405 cm^2 near-miss area) for double coincidence events. The data, which contain no candidate events, set an upper limit of $3.7 \times 10^{-11} \text{ cm}^{-2} \text{ sec}^{-1} \text{ sr}^{-1}$ (90% C.L.) for monopoles of any mass and at any velocity passing through the Earth's surface.

PACS numbers: 14.80.Hv, 94.40.Lx

A Dirac magnetic charge g passing through a superconducting ring changes the magnetic flux threading the ring by exactly $2\Phi_0$, where $\Phi_0 = 2.07 \times 10^{-7} \text{ G cm}^2$ is the flux quantum of superconductivity and $4\pi g = 2\Phi_0$ is the magnetic flux emanating from the monopole. Superconductive detectors based on this property directly measure the magnetic charge of a passing particle independent of its velocity, mass, electric charge, and magnetic dipole moment. The detector response follows from simple and fundamental theoretical considerations.¹ Such detectors are thus natural choices in the search for any flux of cosmic-ray magnetic charges, particularly the nonrelativistic and supermassive monopoles predicted by grand unification theories.²

One of us reported previously on the operation of a single-loop superconductive detector.¹ Those data set an upper limit of $6.1 \times 10^{-10} \text{ cm}^{-2} \text{ s}^{-1} \text{ sr}^{-1} = (\int dA d\Omega dt)^{-1}$ on the monopole particle flux and included one uncorroborated candidate event.³ Other less direct techniques which detect ionization or scintillation have been used to place various velocity-dependent upper limits.⁴ We are now operating a three-loop superconductive detector with a larger sensing area and with sufficient redundancy and cross checks to rule out spurious events. Here we report on the first five months of low-noise operation.

The detection apparatus (Fig. 1) consists of three independent superconducting coils, each made of two turns of $125\text{-}\mu\text{m}$ -diam NbTi wire wound on a hollow 10.2-cm -diam Pyrex sphere. They form mutually orthogonal concentric circles oriented with threefold rotational symmetry about the vertical axis. A two-turn calibration coil, also concentric with the loops, is mounted on the same Pyrex sphere with its axis vertical.

This loop assembly is mounted in an evacuated Pyrex chamber and connected to shielded SQUID sensors located above the vacuum compartment. During cryogenic operation, the detector loops

are surrounded by a cylindrical superconducting shield. The shield is 20 cm in diam by 100 cm long and closed at the bottom with the loops axially centered 71 cm from the top. Ambient magnetic field in the detection region is $\approx 20 \text{ nG}$. Sensitivity to external field variations is further reduced by continuously degaussing a high-permeability magnetic shield which surrounds the Dewar. The combined shielding provides 160 dB attenuation of external magnetic field variations.

The mutual inductance between the two-turn calibration coil and each detector loop ($0.0778 \mu\text{H}$ per detector turn) has been calculated to better than 1% .⁵ Supercurrents induced in the shield walls have been included in the calculation and cause a 6% reduction in the unshielded result. A

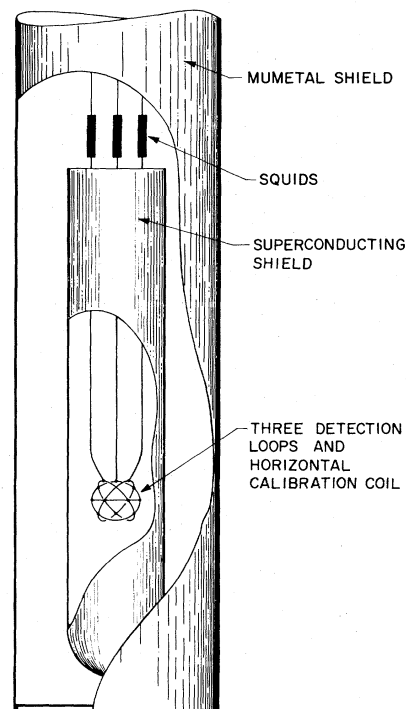


FIG. 1. Schematic of three-loop detector.

current of 53.2 nA in the calibration coil induces supercurrent changes of $4\Phi_0/L$ in all three loops. The measured mutual inductance between any two detector loops is $\approx 10^{-3}L$, where $L \approx 4 \mu\text{H}$ is the total inductance of each detector circuit comprised of the detection loop and the SQUID input coil connected to it. Thus, a current change occurring in only one loop, comparable to that induced by the passage of a Dirac charge, causes no measurable current changes in the other two.

To guard against spurious signals, additional instruments monitor parameters known to affect the detector. A flux-gate magnetometer monitors the external field variations, a pressure transducer measures the helium gas pressure above the bath in the Dewar, an accelerometer detects any mechanical motion of the apparatus along the vertical axis, and a power-line voltage monitor detects six different line-noise and fault conditions.

The output signals from the flux gate, the accelerometer, and the three independent SQUID loop current sensors are sampled continuously at 200 readings per second per channel (100 Hz bandwidth) with a computer data-acquisition system. These data are temporarily stored in the computer memory as a circular buffer and digitally filtered to 0.1 Hz bandwidth (one point every 5 s) in real time. The filtered data and readings taken every 5 s from the pressure sensor and the line voltage monitor are stored to form a permanent record. In addition, successive filtered data are constantly compared to detect sudden changes in the SQUID sensor levels above a threshold of $0.3\Phi_0/L$. Such an event triggers the permanent storage of 50 s of high-bandwidth data, beginning with the circular buffer which always contains from 12.5 to 25 s of data prior to the event. Such high-bandwidth data are particularly useful for detecting mechanically induced disturbances, but would not resolve the supercurrent rise times produced by the passage of a cosmic-ray monopole.

The response of our three-loop detector has been characterized by a detailed calculation which simulates an isotropic distribution of monopole trajectories through the apparatus.⁵ A trajectory which passes through a loop changes the flux threading it by exactly $4\Phi_0$ ($2\Phi_0$ per turn). However, in computation of the induced supercurrent, the cylindrical superconducting shield surrounding the loops must be considered since a Dirac charge would leave doubly quantized supercurrent vortices of opposite polarity at the intersection

of its trajectory with the shield walls. For each of 10^6 simulated monopole trajectories the current changes induced in each loop were found by combining the direct coupling of the particle to that loop (exactly $4\Phi_0/L$ or zero) together with the field from the induced wall vortices coupling to that same loop.

This Monte Carlo calculation was used to find the density of sensing-area function in a three-dimensional signal space in which each point represents an event with coordinates corresponding to the induced supercurrent changes in the three loops. The signal space was partitioned into cubes each $0.1\Phi_0/L$ on an edge and the number of events falling within each cube were counted. The totals were then normalized to give the sensing area density in units of $\text{cm}^2/(\Phi_0/L)^3$. A slice through the resultant distribution function is shown in Fig. 2. Every cube which contained at least one event has been marked and the darker shadings correspond to higher sensing-area densities. Trajectories that intersect at least one loop correspond to the noncentral regions in the distribution function and total 71.2 cm^2 of sensing area averaged over 4π solid angle. The central region corresponds to near-miss trajectories which traverse the shield but do not intersect any loop. This category provides an additional average sensing area of 535 cm^2 for those events which produce signals greater than our threshold of $0.1\Phi_0/L$. Such trajectories pass within one shield diameter of the loop assembly center.

To discriminate better against spurious events,

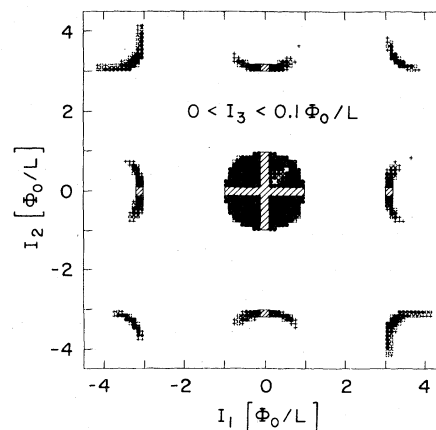


FIG. 2. Slice through density of sensing-area distribution function. Darker regions correspond to higher densities and hatched areas are removed by the double-coincidence requirement.

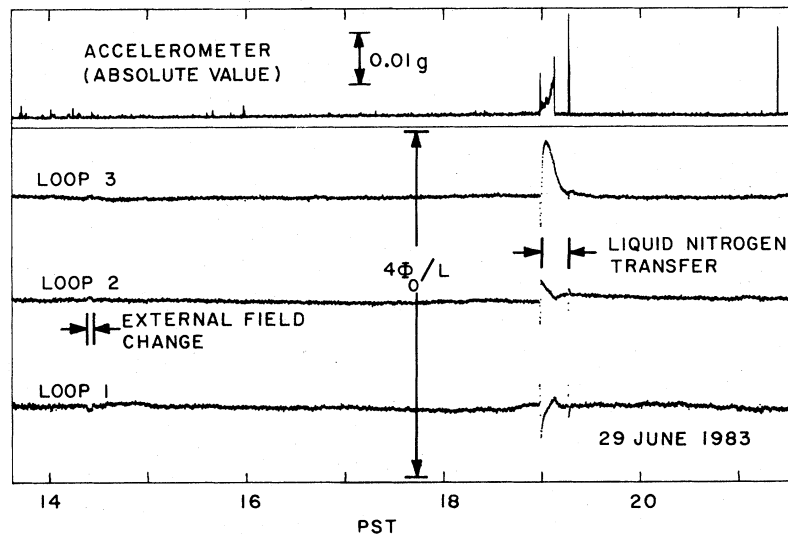


FIG. 3. Typical data record from computer.

we require a signal level greater than $0.1\Phi_0/L$ in at least two of the three loops, reducing the average loop sensing area to 70.5 cm^2 and the near-miss area to 405 cm^2 . This requirement is equivalent to throwing out events within $\pm 0.1\Phi_0/L$ of each axis in the distribution function, as indicated by the hatched areas in Fig. 2. All events in the distribution function are contained within a circumscribed sphere of radius $6.5\Phi_0/L$ which is concentric with the signal space origin. Events passing through at least one loop and satisfying the double-coincidence requirement occupy less than 1% of the sphere's volume. An event in this category not coincident with any disturbance found with our auxiliary instrumentation would provide strong evidence for the existence of magnetic charges. A near-miss event would not provide definitive identification, because the smaller signals are closer to noise levels. However, if no candidates are found, this additional sensing area can be used to set reduced upper bounds on the particle flux.

Since cooldown on 25 January 1983 the three-loop apparatus has been operating continuously with rms noise levels below $0.02\Phi_0/L$ in a 0.1-Hz bandwidth for all three loops—a magnetic field sensitivity of 20 pG. This low-noise operation allows clear detection of signals above the $0.1\Phi_0/L$ threshold. As of 30 June 1983 we have accumulated 129.6 days of data on the computer, surpassing the area-time reported for any other superconductive detector. Figure 3 contains a data segment which includes a typical disturbance from a liquid-nitrogen transfer and one from a

truck temporarily parked at a nearby loading dock. Not shown are other easily identifiable routine disturbances caused by manual offset adjustments, by large magnetic objects moved near the apparatus (liquid-nitrogen Dewars and vacuum pumping station), and by changes in the helium recovery-line pressure.

To analyze the recorded data, we have developed an algorithm that searches for offsets occurring above a threshold of $0.1\Phi_0/L$ while ignoring slow changes and brief excursions above threshold which quickly return to their previous value. The digital filter used in the real-time computer data-acquisition system has a step-function response given by $V(t) = V_{\text{initial}} + V_{\text{step}}(1 - e^{-t/\tau})$ where $\tau = 5/\pi = 1.59 \text{ s}$. Thus after three filtered data points (15 s) the output is within 99.8% of the full step change. The data-scanning algorithm searches for offsets above threshold, jumps two points ahead, and determines whether the data have leveled off. Our criteria require that 100 points of data (500 s) all remain within $\pm 0.1\Phi_0/L$ of their initial value both before and after the three-point transient. The active detection time is obtained by subtracting the vetoed intervals from the total.

This algorithm successfully identifies offsets that are apparent in a visual scan of the data and ignores slow-moving changes, for instance those caused by nitrogen and helium transfers. Histograms of events found by the algorithm in the 129.6-day record (121.5 days of active operation) are shown in Fig. 4. Events from known causes, determined by peripheral instrumentation and

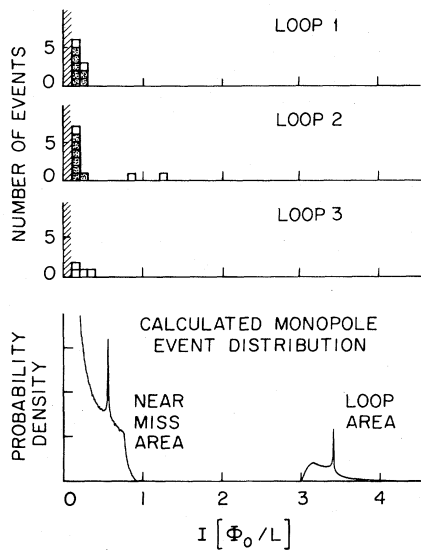


FIG. 4. Histograms of events above threshold prior to elimination by coincidence veto. Unshaded events occurred within the first 5 days after cooldown. The single-loop distribution function for monopole events is included for calibration (Ref. 5).

logged annotations, are not included. No vetos based exclusively on the accelerometer data have been necessary. We do not know the direct causes for those that remain, but many occurred within the first 5 days (unshaded events in Fig. 4) during a settling period of generally noisy data.⁶ No events satisfy the double-coincidence requirement (± 5 -s window), removing them all from consideration as monopole candidates. If we assume uncorrelated rates obtained from data after the first 5 days, accidental double coincidences would occur about every 5000 yr.

In conclusion, these data set an upper limit of $3.7 \times 10^{-11} \text{ cm}^{-2} \text{ s}^{-1} \text{ sr}^{-1}$ at 90% C.L. ($2.3/\int dA d\Omega dt$)

on any uniform flux of magnetic monopoles passing through the Earth's surface at any velocity. No large spurious or real signals were seen, casting no new light on the origin of the previously reported candidate. However, these data lower that previous flux limit¹ by a factor of 38, increasing the probability of a spurious cause for that event.

We intend to continue operating this detector for at least a year. We are also designing a larger detector.

We wish to thank M. Huber and S. B. Felch for technical assistance and R. Huckaby for constructing the Pyrex coil form assembly. This work has been funded by U.S. Department of Energy Contract No. DE-AM03-76SF00-326 and a capital equipment supplement from National Science Foundation Grant No. DMR 80-26007.

¹B. Cabrera, Phys. Rev. Lett. **48**, 1378 (1982), and references therein.

²For a recent detailed review of theory and experiment, see *Magnetic Monopoles*, edited by R. A. Carrigan and W. P. Trower (Plenum, New York, 1983).

³See B. Cabrera, in Ref. 2; J. F. Ziegler, C. C. Tsuei, C. C. Chi, C. D. Tesche, P. Chandhari, and K. W. Jones, Phys. Rev. D **28**, 1793 (1983).

⁴See G. Giacomelli, in Ref. 2; and S. P. Ahlen, *ibid.* More recently, see D. E. Groom *et al.*, Phys. Rev. Lett. **50**, 573 (1983); S. P. Ahlen, T. M. Liss, and G. Tarlé, Phys. Rev. Lett. **51**, 940(C) (1983); D. E. Groom *et al.*, Phys. Rev. Lett. **51**, 941(C) (1983); S. Errede *et al.*, Phys. Rev. Lett. **51**, 245 (1983); R. Bonarelli *et al.*, Phys. Lett. **126B**, 137 (1983); J. Bartelt *et al.*, Phys. Rev. Lett. **50**, 655 (1983).

⁵B. Cabrera, R. Gardner, and R. King, to be published.

⁶Recent elimination of cold-solder joints in the loop-2 SQUID electronics has improved its stability.